A Highly Ordered Self-Assembled Monolayer Film of an Azobenzenealkanethiol on Au(111): Electrochemical Properties and Structural Characterization by Synchrotron in-Plane X-ray Diffraction, Atomic Force Microscopy, and Surface-Enhanced Raman Spectroscopy

W. Brett Caldwell,[†] Dean J. Campbell,[†] Kaimin Chen,[†] Brian R. Herr,[†] Chad A. Mirkin,*[,†,⊥] A. Malik,[‡] M. K. Durbin,[‡] P. Dutta,[‡] and K. G. Huang[§]

Contribution from the Department of Chemistry and Department of Physics and Astronomy, Northwestern University, 2145 Sheridan Road, Evanston, Illinois 60208, and Materials Science Division, Argonne National Laboratory, Argonne, Illinois 60439

Received November 2, 1994[⊗]

Abstract: The synthesis and characterization of p-$HS(CH_2)_{11}OC_6H_4N{=}NC_6H_5$, compound **1d**, is reported. Compound **1d** self-assembles onto Au(111) substrates into highly ordered monolayer films. Self-assembled monolayer films (SAMs) of **1d** on Au(111)/mica have been characterized by ellipsometry, surface-enhanced Raman spectroscopy (SERS), and atomic force microscopy (AFM). We also report the characterization of SAMs of **1d** on bulk single crystal Au(111) by synchrotron in-plane X-ray diffraction (XRD) measurements. AFM and in-plane XRD suggest that a SAM of **1d** is comprised of domains of **1d** which form a hexagonal lattice (4.50 ± 0.06 Å nearest neighbor spacing) that is incommensurate with the underlying Au(111) lattice. A model is proposed to describe the SAM structure. In such a model, small bundles (~80 molecules) of ordered azobenzene moieties that rest over a set of inward tilting alkyl surface tethering groups make up the individual domains. The "bundle model" for a SAM of **1d** on Au(111) is a new one and provides insight into the way adsorbate molecules may arrange themselves in these novel materials. Thermal annealing of the as-deposited SAM of **1d** results in a modest increase in domain size from ~45 to ~55 Å and a change in azobenzene tilt angle from 20−30° to approximately 0° with no change in nearest neighbor spacing. The redox activity of the azobenzene group is significantly affected by monolayer film structure. Only 2% of the azobenzene groups within a SAM of **1d** are electrochemically accessible through cyclic voltammetry in a THF/0.1 M n-Bu_4NPF_6 electrolyte. The monolayer structure impedes the incorporation of charge compensating ions into the film, thereby regulating the electrochemical accessibility of the azobenzene redox centers within the film. Submonolayer films of **1d** and films prepared by the coadsorption of **1d** with ethanethiol on Au(111)/mica have greater electrochemical accessibilities with regard to the azobenzene groups than do pure SAMs of **1d**. Interfacial capacitance measurements and film penetration studies with $Fe(CN)_6^{3-}$ show that SAMs of **1d** are densely packed structures which form impenetrable barriers to $Fe(CN)_6^{3-}$.

Introduction

Spontaneously adsorbed monolayer films have received a great deal of attention for their enormous potential in tailoring surface properties for a variety of technologically important applications. Such films have been used in the design of interfaces for chemical sensing applications,[1] nonlinear optical materials,[1a,2] surfaces for photopatterning methodology,[3] and optically sensitive interfaces for proof-of-concept molecule-based actinometers and high density memory devices.[1a,4] In addition, spontaneously adsorbed monolayer films have been used to study important fundamental processes involving interfacial electron transfer, adhesion, and surface wetting.[5] Thus far, the spontaneous adsorption of monolayer films has been demonstrated for a wide range of adsorbate functional groups and substrates; some of these include thiols,[5] disulfides,[6] sulfides,[7] and phosphines[8a] on Au, carboxylic acids on metal

* Author to whom correspondence should be addressed.
† Department of Chemistry, Northwestern University.
‡ Department of Physics and Astronomy, Northwestern University.
§ Argonne National Laboratory.
⊥ Dreyfus Foundation New Faculty Awardee (1991−1996), Beckman Young Investigator (1992−1994), National Science Foundation Young Investigator (1993−1998), Naval Young Investigator (1994−1997), A. P. Sloan Foundation Fellowship.

⊗ Abstract published in *Advance ACS Abstracts,* May 1, 1995.

(1) (a) Mirkin, C. A.; Ratner, M. A. *Annu. Rev. Phys. Chem.* **1992**, *43*, 719. (b) Mirkin, C. A.; Valentine, J. R.; Ofer, D.; Hickman, J. J.; Wrighton, M. S. In *Biosensors and Chemical Sensors*; Edelman, P. G., Wang, J., Eds.; ACS Symposium Series 487, American Chemical Society: Washington, DC, 1992; Chapter 17. (c) Hickman, J. J.; Ofer, D.; Laibinis, P. E.; Whitesides, G. M.; Wrighton, M. S. *Science* **1991**, *252*, 688.

(2) Li, D.; Ratner, M. A.; Marks, T. J.; Zhang, C. H.; Yang, J.; Wong, G. K *J. Am. Chem. Soc.* **1990**, *112*, 7389.

(3) (a) Wollman, E. W.; Kang, D.; Frisbie, C. D.; Lorkovic, I. M.; Wrighton, M. S. *J. Am. Chem. Soc.* **1994**, *116*, 4395. (b) Wollman, E. W.; Frisbie, C. D; Wrighton, M. S. *Langmuir* **1993**, *9*, 1517. (c) Tarlov, M. J.; Burgess, D. R. F., Jr.; Gillen, G. *J. Am. Chem. Soc.* **1993**, *115*, 5305.

(4) (a) Kawanishi, Y.; Tamaki, T.; Sakuragi, M.; Seki, T.; Suzuki, Y.; Ichimura, K. *Langmuir* **1992**, *8*, 2601. (b) Ichimura, K.; Suzuki, Y.; Seki, T.; Hosoki, A.; Aoki, K. *Langmuir* **1988**, *4*, 1214.

(5) For reviews on monolayer films, see: (a) Bain, C. D.; Whitesides, G. M. *Angew. Chem., Int. Ed. Engl.* **1989**, *28*, 506. (b) Dubois, L. H.; Nuzzo, R. G. *Annu. Rev. Phys. Chem.* **1992**, *43*, 437. For additional manuscripts describing electron transfer phenomena in monolayer films see: (c) Finklea, H. O.; Avery, S.; Lynch, M.; Furtsch, T. *Langmuir* **1987**, *3*, 409. (d) Finklea, H. O.; Hanshew, D. D. *J. Am. Chem. Soc.* **1992**, *114*, 3173. (e) Chidsey, C. E. D. *Science* **1991**, *251*, 919. (f) Tender, L.; Carter, M. T.; Murray, R. W. *Anal. Chem.* **1994**, *66*, 3173. (g) Weber, K.; Creager, S. E. *Anal. Chem.* **1994**, *66*, 3164. (h) Li, T. T. T.; Weaver, M. J. *J. Am. Chem. Soc.* **1984**, *106*, 6107. (i) Creager, S. E.; Weber, K. *Langmuir* **1993**, *9*, 844. (j) Lenhard, J. R.; Murray, R. W. *J. Am. Chem. Soc.* **1978**, *100*, 7870.

(6) (a) Nuzzo, R. G.; Allara, D. L. *J. Am. Chem. Soc.* **1983**, *105*, 4481. (b) Nuzzo, R. G.; Fusco, F. A.; Allara, D. L. *J. Am. Chem. Soc.* **1987**, *109*, 2358.

0002-7863/95/1517-6071$09.00/0

oxides,[9] trichloro- and trialkoxysilanes on oxide surfaces,[10a] thiols and alkylamines on high temperature superconductor surfaces,[10b] phosphonates on metal phosphonate surfaces,[11] thiols on GaAs,[12a] CdSe,[12b] CdS,[12b] Cu,[13] and Ag,[13] and thiols,[8] olefins,[14a,b] and isonitriles[14c,d] on Pt.

Some adsorbate molecules not only form strong chemical bonds with surfaces but also self-organize into highly ordered structures. These structures are referred to as self-assembled monolayers (SAMs). The best characterized SAMs are those formed from the adsorption of long chain linear alkanethiols on noble metal substrates such as Au(111), Au(100), and Ag-(111)[5b] and linear alkane chloro- or alkoxysilanes adsorbed onto oxide coated Si substrates.[15] Self-assembly of linear alkanethiols onto Au(111) substrates has been the most extensively studied system. The structure for SAMs of *n*-alkanethiols on Au(111) has been studied by in-plane X-ray diffraction (XRD),[16a-d] helium diffraction,[16c,17] atomic force microscopy (AFM),[18] scanning tunneling microscopy (STM),[19] low energy electron diffraction (LEED),[20] and reflection-absorption infrared spectroscopy.[5b] Most data thus far are consistent with a ($\sqrt{3} \times \sqrt{3}$) R30° structure that is commensurate with the underlying Au(111) substrate, Figure 1. In such a model, each alkyl group may rest over a 3-fold hollow site on the underlying Au-(111) face. The nature of the surface attachment is believed by many to involve a Au-thiolate interaction;[5] however, it should be noted that some workers recently have invoked the possibility of the RS groups dimerizing on the surface to form disulfides.[16d] Shorter chain linear alkanethiols are believed to have a similar structure,[18,19] but the extent of order decreases as chain length decreases.[10]

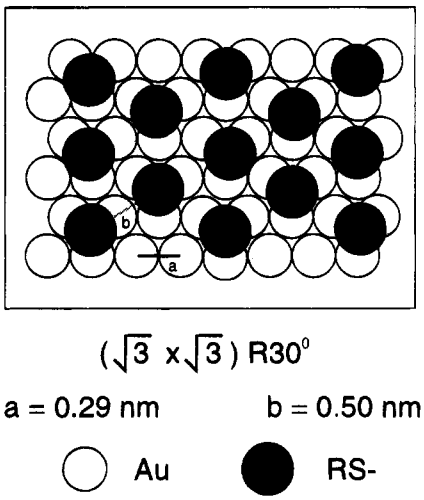

Figure 1. An illustration of a ($\sqrt{3} \times \sqrt{3}$) R30° structure for a linear alkanethiol SAM on Au(111).

In spite of over a decade of work aimed at preparing and characterizing SAMs, there still is not a clear understanding of the factors that govern the self-assembly process. Questions pertaining to the relative importance of adsorbate–surface interactions, intermolecular interactions, molecular shape, and kinetic barriers to surface mobility remain unanswered. In short, it is difficult to predict what types of molecules will or will not form highly organized structures on surfaces that vary in chemical composition and crystal type. The answers to these questions rely on the synthesis of new self-assembling adsorbate molecules, a clearer understanding of surface coordination chemistry, and state-of-the art surface-analytical techniques (e.g., synchrotron in-plane XRD, AFM, STM, etc.) for characterizing monolayer structures.

The term "self-assembled monolayer" is a vague one. It carries with it two major implications: (1) the formation of a monolayer film through the spontaneous chemical adsorption of adsorbate molecules and (2) order that arises from secondary interactions between adsorbate molecules that comprise the film. Spontaneous adsorption differentiates SAMs from Langmuir–Blodgett (LB) films, which are a class of ordered monolayers that are physisorbed rather than chemisorbed structures.[10] *Order* is a relative term, and with regard to spontaneously adsorbed monolayer films, it has been used somewhat indiscriminately by many throughout the literature. By definition, when a molecule is adsorbed onto a surface, order has been imparted into the system; an adsorbed molecule has fewer degrees of freedom than does the same molecule in solution. Therefore, throughout the literature, monolayer films that are spontaneously adsorbed onto a substrate are often referred to as SAMs with no clear indication of the extent of order. Our operating definition of highly ordered is a film which diffracts X-rays or exhibits a distinct lattice that can be imaged via a scanning probe microscopy. Indeed, if one rigorously defines a SAM as a highly ordered monolayer that is formed from the spontaneous adsorption of adsorbate molecules from solution or the gas phase, there are very few systems that have definitively been shown to fall into this category. In fact, linear alkanes (both fluoro-[16e,f] and hydrocarbon[15,16a-d,17-20]) and, recently, fullerenes[21] with surface attaching functional groups are the only classes of

(7) Troughton, E. B.; Bain, C. D.; Whitesides, G. M.; Nuzzo, R. G.; Allara, D. L.; Porter, M. D. *Langmuir* **1988**, *4*, 365.

(8) (a) Lee, T. R.; Laibinis, P. E.; Folkers, J. P.; Whitesides, G. M. *Pure Appl. Chem.* **1991**, *63*, 821. (b) Gui, J. Y.; Stern, D. A.; Frank, D. G.; Lu, F.; Zapien, D. C.; Hubbard, A. T. *Langmuir* **1991**, *7*, 955.

(9) (a) Allara, D. L.; Nuzzo, R. G. *Langmuir* **1985**, *1*, 45. (b) Allara, D. L.; Nuzzo, R. G. *Langmuir* **1985**, *1*, 52.

(10) (a) For a review, see: Ulman, A. *An Introduction to Ultrathin Organic Films: From Langmuir-Blodgett to Self-assembly*, Academic Press: Boston, 1991. (b) Chen, K.; Mirkin, C. A.; Lo, R.-K.; Zhao, J.; McDevitt, J. T. *J. Am. Chem. Soc.*, in press.

(11) Lee, H.; Kepley, L. J.; Hong, H.-G.; Akhter, S.; Mallouk, T. E. *J. Phys. Chem.* **1988**, *92*, 2597.

(12) (a) Sheen, C. W.; Shi, J.-X.; Martensson, J.; Parikh, A. N.; Allara, D. L. *J. Am. Chem. Soc.* **1992**, *114*, 1514. (b) Natan, M. J.; Thackeray, J. W.; Wrighton, M. S. *J. Phys. Chem.* **1986**, *90*, 4089.

(13) (a) Laibinis, P. E.; Whitesides, G. M. *J. Am. Chem. Soc.* **1992**, *114*, 1990. (b) Laibinis, P. E.; Whitesides, G. M.; Allara, D. L.; Tao, Y.-T.; Parikh, A. N.; Nuzzo, R. G. *J. Am. Chem. Soc.* **1991**, *113*, 7152.

(14) (a) Lane, R. F.; Hubbard, A. T. *J. Phys. Chem.* **1973**, *77*, 1401. (b) Lane, R. F.; Hubbard, A. T. *J. Phys. Chem.* **1973**, *77*, 1411. (c) Hickman, J. J.; Zou, C.; Ofer, D.; Harvey, P. D.; Wrighton, M. S.; Laibinis, P. E.; Bain, C. D.; Whitesides, G. M. *J. Am. Chem. Soc.* **1989**, *111*, 7271. (d) Hickman, J. J.; Laibinis, P. E.; Auerbach, D. I.; Zou, C.; Gardner, T. J.; Whitesides, G. M.; Wrighton, M. S. *Langmuir* **1992**, *8*, 357.

(15) (a) Pomerantz, M.; Segmüller, A.; Netzer, L.; Sagiv, J. *Thin Solid Films* **1985**, *132*, 153. (b) Wasserman, S. R.; Whitesides, G. M.; Tidswell, I. M.; Ocko, B. M.; Pershan, P. S.; Axe, J. D. *J. Am. Chem. Soc.* **1989**, *111*, 5852. (c) Tidswell, I. M.; Ocko, B. M.; Pershan, P. S.; Wasserman, S. R.; Whitesides, G. M.; Axe, J. D. *Phys. Rev. B* **1990**, *41*, 1111. (d) Tidswell, I. M.; Rabedeau, T. A.; Pershan, P. S.; Kosowsky, S. D.; Folkers, J. P.; Whitesides, G. M. *J. Chem. Phys.* **1991**, *95*, 2854.

(16) (a) Samant, M. G.; Brown, C. A.; Gordon, J. G., II. *Langmuir* **1991**, *7*, 437. (b) Fenter, P.; Eisenberger, P.; Liang, K. S. *Phys. Rev. Lett.* **1993**, *70*, 2447. (c) Camillone, N., III; Chidsey, C. E. D.; Eisenberger, P.; Fenter, P.; Li, J.; Liang, K. S.; Liu, G.-Y.; Scoles, G. *J. Chem. Phys.* **1993**, *99*, 744. (d) Fenter, P.; Eberhardt, A.; Eisenberger, P. *Science* **1994**, *266*, 1216. (e) Alves, C. A.; Porter, M. D. *Langmuir* **1993**, *9*, 3507. (f) Liu, G. -Y.; Fenter, P.; Chidsey, C. E. D.; Ogletree, D. F.; Eisenberger, P.; Salmeron, M. *J. Chem. Phys.* **1994**, *101*, 4301.

(17) (a) Camillone, N., III; Chidsey, C. E. D.; Liu, G.-Y.; Putvinski, T. M.; Scoles, G. *J. Chem. Phys.* **1991**, *94*, 8493. (b) Camillone, N., III; Chidsey, C. E. D.; Liu, G.-Y; Scoles, G. *J. Chem. Phys.* **1993**, *98*, 3503. (c) Camillone, N., III; Chidsey, C. E. D.; Liu, G.-Y.; Scoles, G. *J. Chem. Phys.* **1993**, *98*, 4234.

(18) Alves, C. A.; Smith, E. L.; Porter, M. D. *J. Am. Chem. Soc.* **1992**, *114*, 1222.

(19) Widrig, C. A.; Alves, C. A.; Porter, M. D. *J. Am. Chem. Soc.* **1991**, *113*, 2805.

(20) (a) Strong, L.; Whitesides, G. M. *Langmuir* **1988**, *4*, 546. (b) Dubois, L. H.; Zegarski, B. R.; Nuzzo, R. G. *J. Chem. Phys.* **1993**, *98*, 678.

(21) Shi, X.; Caldwell, W. B.; Chen, K.; Mirkin, C. A. *J. Am. Chem. Soc.* **1994**, *116*, 11598.

well characterized molecules that have definitively been shown to form SAMs with a distinct degree of order as determined from in-plane XRD or scanning probe microscopy experiments.

Another important set of issues regarding SAMs, and spontaneously adsorbed monolayer films in general, pertains to the chemical and physical consequences of adsorbate surface attachment, dense packing, and self-organization. In this regard, there is a series of relevant questions. First, are *significantly* more stable films obtained from highly ordered monolayer structures, and is this an adsorbate general phenomenon? From the work performed on linear alkanethiols adsorbed onto noble metal substrates, it is evident that the SAMs formed from the long chain linear alkanethiols are less susceptible to exchange reactions with adsorbate molecules in solution than SAMs of their short chain counterparts.[22,23] Second, how are chemical reactions affected by SAM structure; are there new reactions that can be realized within the context of a SAM that are not characteristic of the solution forms of the adsorbate molecules? Third, how are electron transfer processes affected by monolayer structure? The use of SAM methodology in the *rational* construction of molecule-based devices relies on a clear understanding of the chemical and physical consequences of the self-assembly process. Although linear alkanethiols (both fluoro- and hydrocarbon) form highly ordered SAMs, they are not very chemically reactive and do not possess redox-active functionalities. In order to answer the aforementioned questions, one must prepare new adsorbate molecules with chemically reactive and redox-active functionalities. The challenge is to select a functional group that has one or more of these characteristics and which is conducive to the formation of highly ordered SAMs.

Herein, we report the synthesis and characterization of one such molecule, *p*-$HS(CH_2)_{11}OC_6H_4N{=}NC_6H_5$ (**1d**), and its spontaneous self-assembly into highly ordered SAMs on Au(111)/mica and bulk single crystal Au(111) substrates. We show that the azobenzene group plays a critical role in SAM formation and that the structure of the SAM, which has been characterized by synchrotron in-plane XRD, AFM, ellipsometry, surface-enhanced Raman spectroscopy (SERS), and electrochemistry, controls the redox properties of the azobenzene units that comprise the film. This study builds on the growing body of work regarding the use of the azobenzene moiety to form organized materials such as liquid crystals,[24] LB films,[25,26] and polymer-based materials for photonic and molecule-based electronic device applications.[27] Others have chemically modified *oxide* surfaces with azobenzene-based molecules; however, the focus of their studies was device oriented and not primarily aimed at elucidating monolayer structure.[4]

Au(111) and compound **1d** were selected for these studies for the following reasons: (1) Au(111) substrates with large atomically flat terraces may be prepared by thermal evaporation of Au onto mica,[28] (2) Au(111) may be used as an electrode to electrochemically characterize redox-active adsorbate molecules, (3) our Au(111)/mica substrates are SERS-active at $\lambda_{ex} = 752$ nm with enhancement factors of $\sim 10^3 - 10^4$,[28a] and the azobenzene group is a large-cross section Raman tag,[29] making characterization of SAMs by Raman spectroscopy straightforward,[28a] (4) the SH group in **1d** allows for its adsorption onto Au substrates, (5) *trans*-azobenzene is a planar sheet-like moiety that has a propensity to crystallize, and (6) the *trans*-azobenzene group is chemically reactive and redox-active; therefore, if SAMs can be prepared from **1d**, chemical and electron transfer reactions may be studied in the context of a SAM. In this study, we focus on the structural characterization of a monolayer prepared from **1d** and the relationship between film structure and electron transfer processes between the Au electrode surface and redox centers in the film and in solution in contact with the film.

Experimental Section

General Methods. All manipulations were performed air-free using Schlenk techniques unless otherwise noted. Absolute ethanol was purchased from Midwest Grain Products, Pekin, IL. Ethanethiol, octadecanethiol, potassium hydroxide, potassium thioacetate, tetra-*n*-butylammonium hexafluorophosphate, sodium perchlorate, and potassium ferricyanide were purchased from Aldrich Chemical Company. Tetra-*n*-butylammonium hexafluorophosphate was recrystallized three times from ethanol, and sodium perchlorate was recrystallized from ethanol prior to use. Methanesulfonyl chloride was purchased from Aldrich Chemical Company and was distilled prior to use. Triethylamine was purchased from Aldrich Chemical Company and was distilled over KOH. Dichloromethane and pentane were dried by refluxing over CaH_2 while benzene, ether, and tetrahydrofuran were dried by refluxing over Na/benzophenone.[30] All organic solvents were freshly distilled prior to use. Deionized H_2O, EtOH, and HOAc were deoxygenated by bubbling with prepurified grade N_2 for a minimum of 30 min. Red muscovite mica was purchased from Asheville Mica, Newport News, VA. NMR spectra were recorded on a Varian Gemini-300 FT NMR spectrometer, and electron impact (EI) mass spectra were obtained using a Fisions VG 70-250 SE mass spectrometer. Electronic absorption spectra were recorded on a Hewlett-Packard 8452A diode array spectrophotometer, and elemental analyses were obtained from Searle Laboratories, Skokie, IL.

Preparation of Au Substrates. Au(111)/mica was prepared with a Veeco Model VE400 thermal evaporator operating at a base pressure of 10^{-6} Torr and equipped with an Inficon XTC 6 MHz quartz crystal microbalance to control the rate of deposition and measure the mass thickness of the film. Au(111)/mica films were epitaxially grown onto freshly cleaved mica by resistively heating Au wire (99.95%, Aldrich)

(22) (a) Biebuyck, H. A.; Whitesides, G. M. *Langmuir* **1993**, *9*, 1766. (b) Bain, C. D.; Evall, J.; Whitesides, G. M. *J. Am. Chem. Soc.* **1989**, *111*, 7155.

(23) Collard, D. M.; Fox, M. A. *Langmuir* **1991**, *7*, 1192.

(24) (a) Aoki, K.; Tamaki, T.; Seki, T.; Kawanishi, Y.; Ichimura, K. *Langmuir* **1992**, *8*, 1014. (b) Seki, T.; Sakuragi, M.; Kawanishi, Y.; Suzuki, Y.; Tamaki, T.; Ichimura, K.; Fukuda, R.; Hiramatsu, H. *Thin Solid Films* **1992**, *210/211*, 836. (c) Sakuragi, M.; Tamaki, T.; Seki, T.; Suzuki, Y.; Kawanishi, Y.; Ichimura, K. *Chem. Lett.* **1992**, 1763. d) Anderle, K.; Birenheide, R.; Werner, M. J. A.; Wendorff, J. H. *Liquid Crystals* **1991**, *9*, 691. (e) Anderle, K.; Birenheide, R.; Eich, M.; Wendorff, J. H. *Makromol. Chem., Rapid Commun.* **1989**, *10*, 477.

(25) (a) Maack, J.; Ahuja, R. C.; Möbius, D.; Tachibana, H.; Matsumoto, M. *Thin Solid Films* **1994**, *242*, 122. (b) Fujiwara, I.; Ishibashi, T.; Asai, N. *J. Appl. Phys.* **1994**, *75*, 4759. (c) Morigaki, K.; Liu, Z. F.; Hashimoto, K.; Fujishima, A. *Sensors and Actuators B* **1993**, *13–14*, 226. (d) Liu. Z. F.; Morigaki, K.; Enomoto, T.; Hashimoto, K.; Fujishima, A. *J. Phys. Chem.* **1992**, *96*, 1875. (e) Liu, Z. F.; Morigaki, K.; Hashimoto, K.; Fujishima, A. *Anal. Chem.* **1992**, *64*, 134.

(26) (a) Liu, Z. F.; Hashimoto, K.; Fujishima, A. *Nature* **1990**, *347*, 658. (b) Liu, Z. F.; Loo, B. H.; Hashimoto, K.; Fujishima, A.; *J. Electroanal. Chem.* **1991**, *297*, 133. (c) Liu, Z. F.; Hashimoto, K.; Fujishima, A. *Chem. Lett.* **1990**, 2177.

(27) (a) Sekkat, Z.; Büchel, M.; Orendi, H.; Menzel, H.; Knoll, W. *Chem. Phys. Lett.* **1994**, *220*, 497. (b) Barley, S. H.; Gilbert, A.; Mitchell, G. R. *J. Mater. Chem.* **1991**, *1*, 481. (c) Seki, T.; Tamaki, T.; Suzuki, Y.; Kawanishi, Y.; Ichimura, K.; Aoki, K. *Macromolecules* **1989**, *22*, 3505. (d) Kawanishi, Y.; Tamaki, T.; Seki, T.; Sakuragi, M.; Suzuki, Y.; Ichimura, K.; Aoki, K. *Langmuir* **1991**, *7*, 1314.

(28) (a) Caldwell, W. B.; Chen, K.; Herr, B. R.; Mirkin, C. A.; Hulteen, J. C.; Van Duyne, R. P. *Langmuir* **1994**, *10*, 4109. (b) Chidsey, C. E. D.; Loiacono, D. N.; Sleator, T.; Nakahara, S. *Surf. Sci.* **1988**, *200*, 45. (c) Goss, C. A.; Brumfield, J. C.; Irene, E. A.; Murray, R. W. *Langmuir* **1993**, *9*, 2986.

(29) (a) Womack, J. D.; Vickers, T. J.; Mann, C. K. *Appl. Spectrosc.* **1987**, *41*, 117. (b) Klima, M. I.; Kotov, A. V.; Gribov, L. A. *Zhurnal Strukturnoi Khimii* **1972**, *13*, 987. (c) Kellerer, B.; Hacker, H. H.; Brandmüller, J. *Indian J. Pure & Appl. Phys.* **1971**, *9*, 903. (d) Trotter, P. J. *Appl. Spectrosc.* **1977**, *31*, 31.

(30) Gordon, A. J.; Ford, R. A. *The Chemist's Companion*, John Wiley & Sons: New York, 1972.

in a tungsten boat source (R. D. Mathis, Long Beach, CA) at a deposition rate of 0.03 nm/s and a substrate temperature of 240 °C.

For the X-ray diffraction experiments, we used single crystal Au (99.99+%) substrates from Monocrystals Co., Cleveland, OH. The crystals were one centimeter in diameter and two millimeters thick. The crystals were mechanically polished along the (111) face and then etched, using an aqueous KI(4 M)/I_2(6 M) solution, to remove surface deformities induced during polishing. *Note: This is a caustic solution, and extreme care should be taken to avoid skin contact.* Finally, the crystals were annealed at 800 °C under vacuum in a tube furnace for 7 days.

SAM Preparation. In a typical experiment, freshly prepared Au(111) substrates were immersed for 48 h in a 1 mM cyclohexane solution of **1d** at 22 °C. The wafers were removed from solution, vigorously rinsed with cyclohexane and tetrahydrofuran, and blown dry with prepurified grade N_2 prior to use.

Ellipsometry. A Sopra MOSS ES 4 G spectroscopic ellipsometer was used to determine the film thickness for SAMs of **1d** on Au(111)/mica. Before and after monolayer adsorption, the ellipsometric parameters tan ψ and cos Δ were acquired from 600 to 820 nm at 10 nm intervals at an angle of 75° with respect to the surface normal. Each data point represents an average of three measurements at each λ. In this range, the molecules that comprise the monolayer are transparent; therefore, in fitting the experimental data, the imaginary portion of the refractive index was disregarded ($k = 0$). The real refractive index (n) was assumed to be 1.55, in accordance with the average known values for 4-ethoxyazobenzene (1.64)[31] and undecanethiol (1.45).[32] The data were modeled in the multilayer regression mode with the number of layers set equal to 1 and referenced to an octadecanethiol SAM, which based on literature precedent was assumed to be 23.8 Å thick.[32] The thickness reported for the monolayer is an average of 11 measurements.

Raman Spectroscopy. A Coherent Innova 400 Ar^+ laser was used at $\lambda_{ex} = 501.7$ nm for the solution and solid spectra of **1**. For the SERS experiment, the Ar^+ laser was used to pump a Spectra Physics Tsunami mode locked Ti:Al_2O_3 laser to obtain $\lambda_{ex} = 752$ nm. A band pass filter (Oriel Corporation, Stratford, CT) centered at 750 nm with a 10 nm range was utilized for removing extra lines. Spectra were recorded at $\lambda_{ex} = 501.7$ and 752 nm using a SPEX Model 1877 Triplemate triple grating monochromator equipped with 600 groove/nm gratings blazed at 750 nm in the filter stage, 1200 groove/nm gratings in the spectrograph stage, and a SPEX Spectrum One CCD detector. The angle of incidence of the laser excitation source was ~45° with respect to the surface normal, and Raman scattered light was collected parallel to the surface normal.

AFM Measurements. Images were recorded using a Nanoscope II microscope equipped with a 0.7 μm scan head (Digital Instruments). All images were acquired in air with Si_3N_4 cantilevers having pyramidal tips with 70° cone angles and 20–40 nm nominal tip radii of curvature (R_c). Cantilevers with force constants of 0.58 N/m were used to image the Au(111)/mica film, and ones with force constants of 0.38 N/m were used to image SAMs. The large scan size Au(111)/mica image was acquired in height mode with the total force equal to 20–60 nN and a scan rate of 1.34 lines s^{-1}, while all other images were acquired at a scan rate of 78 lines s^{-1} in force mode with the total force in each experiment equal to 10–20 nN. All images are 400 × 400 pixels and were reproducible even after scanning for 2–3 h. Freshly cleaved mica was imaged as a standard for each measurement, and all images are unfiltered unless otherwise noted.

X-ray Studies. The XRD experiments were performed in the grazing incidence geometry[33a] at the Argonne National Laboratory's Beam Line X-6B[33b] at the National Synchrotron Light Source. For each experiment, the sample was contained in a chamber enclosed by mylar windows. This chamber was mounted onto a Huber 6-circle diffractometer using a vertical translator to position the sample into the beam. The chamber was purged with helium before the X-ray beam was turned on, and a small over-pressure of helium was maintained in the chamber during the experiment to reduce radiation damage. X-rays of energy 8 KeV ($\lambda = 1.55$ Å) were used for this experiment. The X-ray beam was focused by a toroidal mirror[33b] and slit down to a spot size of 0.7 mm × 0.7 mm at the sample. For these experiments the incident angle on the substrate surface was kept constant at 1°. Two factors governed the choice of incident angle. The angle must be close to the critical angle of the substrate (0.45° for gold at the selected wavelength) to reduce background noise from the bulk, and the angle also should be large enough so that the majority of the beam hits the sample. The value of 1° gave the best signal-to-noise ratio. The rod scans are performed both at the peak position and ±0.3 $Å^{-1}$ off the peak. The difference, meaning the counts above background, is plotted without further normalization.

Electrochemical Measurements. Cyclic voltammetry was performed with a Pine AFRDE4 or Pine AFRDE5 bipotentiostat with a Kipp en Zonen BD90 X-Y or Linseis LY 1400 recorder. Aqueous electrochemical experiments were performed under a prepurified Ar atmosphere and nonaqueous electrochemical experiments were performed in a Vacuum Atmospheres glovebox under N_2 atmosphere. A conventional three-electrode cell was used for all electrochemical experiments. Each cell consisted of a Au(111)/mica or a Au disk working electrode, a Pt gauze counter electrode, and a Ag wire or Ag/AgCl reference electrode. In some cases, ferrocene (Fc) was added as an internal reference. Capacitance measurements are based on the current at −0.1 V vs Ag wire with the thickness of the films being derived from the ellipsometry measurements and a refractive index of 1.55.

Results and Discussion

Au(111)/Mica Films. The surface morphology of Au thin films deposited on freshly cleaved mica is extremely dependent upon Au deposition rate, ultimate Au film thickness, substrate temperature, and chamber pressure.[28a] The parameters used for preparation of the Au(111)/mica films used in this study are given in the Experimental Section of this manuscript. Because of the Au surface morphology dependence on deposition parameters, it is important to characterize Au substrates prior to SAM preparation and characterization. In these studies, we utilize AFM to characterize such substrates; all AFM images herein are given in a topview presentation with the lighter areas denoting higher regions and the darker areas representing lower regions. AFM images of the Au(111)/mica substrates used in these studies show that the surface morphology of the substrates consists of flat terraces that account for approximately 80–85% of the geometric surface area and 60–65% of the microscopic surface area (estimated surface roughness factor, R_f 1.35), Figure 2a. The R_f for comparable substrates has been determined in a previous study.[28a] A higher resolution image of a terrace reveals a hexagonal pattern of bright spots with nearest neighbor spacings (3.0 ± 0.2 Å) consistent with a Au(111) lattice, Figure 2b. It should be noted that others have prepared and characterized Au(111)/mica substrates using comparable, but not identical, conditions and methods.[28b,c] Herein, we present the AFM images of Au(111)/mica to show that we are working with substrates with large Au(111) terraces and to provide a basis for comparison with AFM images of SAMs.

Synthetic Route for p-HS$(CH_2)_{11}OC_6H_4N{=}NC_6H_5$, 1d. Compound **1d** is a new compound and was synthesized by the route outlined in Scheme 1. Full characterization of each intermediate is given in the supplemental material. 4-Hydroxyazobenzene was coupled with 11-bromoundecanol via a Williamson ether synthesis to give p-HO$(CH_2)_{11}OC_6H_4N{=}NC_6H_5$, **1a**. Compound **1a** was mesylated with methanesulfonyl chloride to give p-$CH_3SO_3(CH_2)_{11}OC_6H_4N{=}NC_6H_5$, **1b**, which was

(31) *Handbook of Chemistry and Physics*, 70th ed.; CRC Press: Boca Raton, FL, 1989.

(32) Porter, M. D.; Bright, T. B.; Allara, D. L.; Chidsey, C. E. D. *J. Am. Chem. Soc.* **1987**, *109*, 3559.

(33) (a) Robinson, I. K. In *Handbook on Synchrotron Radiation, Vol. III*; Moncton, D. E., Brown, G. S., Eds., N. Holland Publishing: Amsterdam, 1991. (b) Huang, K. G.; Ramanathan, M.; Montano, P. A. *Rev. Sci. Instrum.*, **1995**, *66*, 1688. (c) Huang, K. G.; Gibbs, D.; Zehner, D. M.; Sandy, A. R.; Mochrie, S. G. J. *Phys Rev. Lett.* **1990**, *65*, 3313.

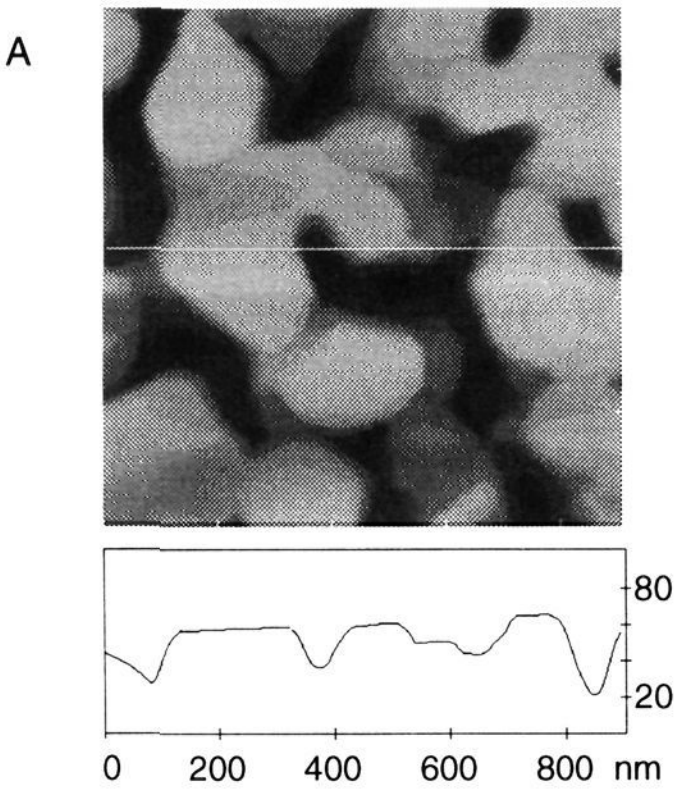

Figure 2. AFM images of a Au(111)/mica film prepared by thermally evaporating Au onto mica. (A) 900 nm × 900 nm scan size image. (B) 8 nm × 8 nm image of a Au(111) lattice.

subsequently thioesterified with potassium thioacetate to form *p*-$CH_3C(O)S(CH_2)_{11}OC_6H_4N{=}NC_6H_5$, **1c**. Deprotection of the thioester group in **1c** with ethanolic KOH with subsequent recrystallization of the crude product gave analytically pure **1d** in 35% overall yield. Gram quantities of **1d** can be prepared routinely from this method.

SAMs of 1d on Au(111)/Mica: Preparation and Characterization by Raman Spectroscopy, Ellipsometry, and Atomic Force Microscopy. Compound **1d** spontaneously self-assembles into highly ordered monolayer films on Au(111)/mica substrates, Scheme 1. The ellipsometrically determined thickness for a SAM of **1d** is 28 ± 1 Å and is consistent with a densely packed monolayer with the adsorbate molecules fully extended from and approximately perpendicular to the Au(111) surface. The length of the fully extended molecule has been estimated to be 27 Å by constructing a model based on crystallographic data for azobenzene and a $C_{11}O$ linear alkanethiol, inset of Scheme 1.[34] We are hesitant about drawing a great deal of structural information from the ellipsometry measurement because it is highly model dependent and typically gives values that are a few Å larger than values determined by more reliable methods such as X-ray reflectivity.[15b] The rms roughness of our substrates precludes the possibility of performing meaningful X-ray reflectivity experiments on them.

The resonance Raman spectra (λ_{ex} = 501.7 nm) of solution **1a** and solid **1a** compare quite well with the SERS spectrum (λ_{ex} = 752 nm) for a SAM of **1d**, Figures 3a–c. These spectra exhibit multiple bands in the 1605–1115 cm^{-1} region, all of which originate from the azobenzene moiety of **1d**.[29] We assign the monolayer spectrum as a SERS spectrum rather than a resonance Raman spectrum or even a surface-enhanced resonance Raman spectrum based on (1) prior work that shows our Au(111)/mica substrates support an $\sim 10^4$ enhancement factor when excited at λ_{ex} = 752 nm[28a] and (2) the UV–vis absorption spectra of **1d** which show λ_{ex} = 752 nm lies well outside the longest wavelength absorption band of **1d** in both the solution and solid states; therefore, it is unlikely that there is a significant resonance contribution to the spectrum of **1d** on Au(111)/mica. Because of the similarity between the solution, solid state, and monolayer Raman spectra of **1** in this spectral region, at this stage it is difficult to extract SAM structural information from such experiments. However, we can conclude that the Au substrate has been modified with compound **1d** and that no unusual chemical reactions with regard to the azobenzene moieties have occurred during the adsorption process. For SAM structural information, we rely on AFM and XRD measurements.

AFM images of SAMs of **1d** on Au(111)/mica in air are consistent with the characterization of a SAM of **1d** as a highly ordered structure, Figures 4a,b. For comparative purposes, we also imaged a SAM of octadecanethiol adsorbed onto Au(111)/mica using similar conditions, Figure 5. Consistent with the work of others,[18] AFM images of a SAM of octadecanethiol adsorbed on Au(111) show a hexagonal array of bright spots with spacings that are significantly larger than those recorded for the Au(111) lattice, compare Figures 2b and 5. The average spacing of 5.1 ± 0.3 Å for the SAM of octadecanethiol on Au(111)/mica is consistent with the expected ($\sqrt{3} \times \sqrt{3}$) R30° structure.

AFM images of SAMs of **1d** on Au(111)/mica (Figure 4) show a slightly distorted hexagonal array of bright spots with spacings that are larger than those attributed to a Au(111) lattice but smaller than those assigned to the lattice formed by a SAM of octadecanethiol, compare Figures 2b, 4b, and 5. Ten independent samples were studied, and the average spacing of 4.6 ± 0.2 Å was reproducible from sample to sample and from scan area to scan area within one sample. A large scan size image (33 nm × 33 nm) shows that the order extends for hundreds of square nanometers, Figure 4a. Consistent with the description of the AFM image of a SAM of **1d** as distorted hexagonal, one set of four spots in a rectangular array can be discerned from a two-dimensional Fourier transform of the image (see supplementary material). The origin of this distortion is most likely an experimental aberration (*vide infra* XRD data). Soft organic films imaged in contact mode are more susceptible to experimentally induced distortions.[21,35d–f] Grain boundaries and domain structure are not apparent in our AFM images of a SAM of **1d**. This is not surprising and is consistent with the

(34) The computer program Sybyl (Tripos Associates, St. Louis, MO) was used to construct a model of **1d**. Crystallographic data for *trans*-azobenzene was used from: Brown, C. J. *Acta Crystallogr.* **1966**, *21*, 146.

Scheme 1

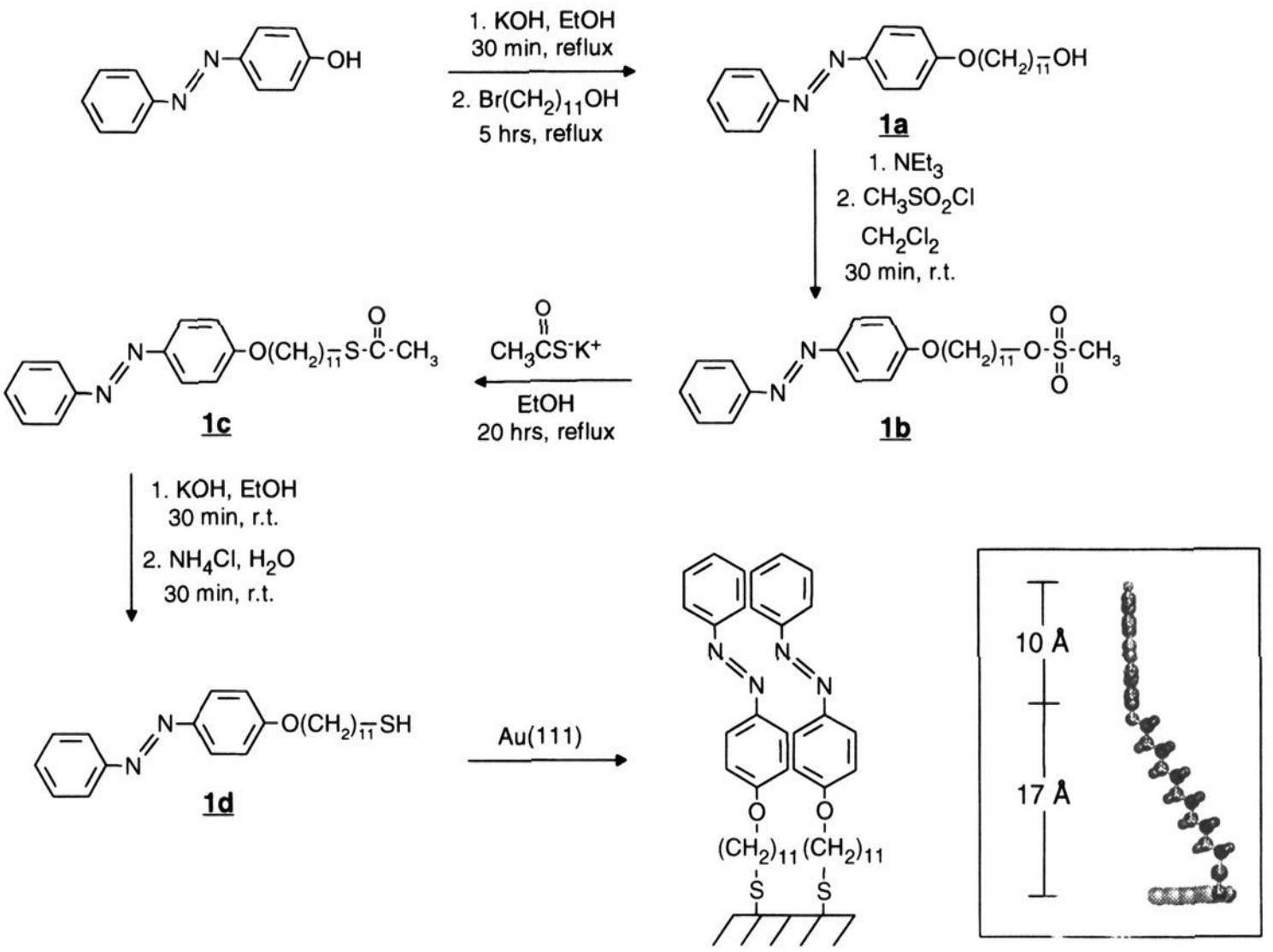

current limitations others have noted for the AFM technique.[35e-i] We are conservative with regard to interpretation of our AFM images and feel that the method, as we use it for organic films under ambient conditions, is a good one for indicating order and extracting estimates for lattice parameters. The lattice parameters extracted from such experiments for four different SAMs (including the one reported herein) correlate well with XRD data (*vide infra*).[15,16,18,21]

In order to make certain that the lattice measured in the AFM experiments for **1d** on Au(111)/mica was monolayer based, an experiment was performed where the monolayer was first imaged at one spot with a ~15 nN force, Figure 6a, and then imaged again in the same spot with increasingly larger forces in an attempt to image the underlying Au(111) lattice. Indeed, when the force was >300 nN a hexagonal lattice with different orientation and spacing than the assigned monolayer lattice was imaged,[35a] Figure 6b; this lattice has a nearest neighbor distance of 3.0 ± 0.2 Å and is offset from the lattice imaged at 15 nN by ~26°.[35b] Note that we are showing the raw data for these images to illustrate their high quality. On the basis of nearest neighbor spacing and relative orientation, these results are consistent with the assignment of the lattice imaged at 15 nN (Figure 6a) to the SAM of **1d** and the lattice imaged at >300 nN (Figure 6b) to the underlying Au(111) face. Others have performed similar force-dependent AFM experiments on SAMs of linear alkanethiols (both hydrocarbon and fluorocarbon) on Au(111)[16f,36] and LB films on mica.[37]

Characterization of a SAM of 1d by in-Plane X-ray Diffraction (XRD). At room temperature, a monolayer diffraction peak for a SAM of **1d** on bulk Au(111) was found at $K_{xy} = 1.61 \pm 0.02$ Å^{-1}, corresponding to a plane spacing of 3.90 ± 0.05 Å in a direction 30° from the Au surface truncation rod (11), Figures 7 (■) and 8a. The peak position is shown in reciprocal space in Figure 9a. While it is not possible to determine the structure uniquely from a single diffraction peak, the absence of other first-order peaks implies that the lattice is hexagonal with a molecular nearest-neighbor distance of 4.50 ± 0.06 Å, Figure 9b. The AFM results discussed earlier are consistent with this model. Given the small lattice parameter and the dimensions of the azobenzene cross section, it is most likely that the azobenzene groups pack in a "herringbone" pattern, Figure 9b. The dimensions of the azobenzene group[34] and the 4.50 ± 0.06 Å hexagonal lattice parameter preclude the possibility of the azobenzene groups forming parallel stacks of face-to-face azobenzene dimers in the SAM. In other words, two nearest neighbor azobenzene groups may not be coplanar and fit into a hexagonal lattice with 4.50 ± 0.06 Å nearest neighbor spacing.

As the film is heated, the diffraction peak intensity gradually decreases as the temperature increases and completely disappears at ~128 °C, Figure 7 (+). Upon cooling the sample, the peak returns to the same position in K_{xy} with comparable intensity and direction with respect to the Au surface truncation rod (11), Figures 7 (▲) and 8b. However, a comparison of the rod scans before and after annealing shows that a structural change has occurred in the SAM, Figure 10. The rod scans are not broad enough to be attributable to scattering from a surface (e.g., a

(35) (a) Depending on the contact area between each tip and the substrate, the total force value may vary. (b) This angle varies slightly from sample to sample with the average value being 29 ± 3°. (c) The cutoff near $K_z = 0$ in the rod scan after annealing is because at very small incident angles a smaller cross section of the X-ray beam is intercepted by the surface. For references which address the current limitations of AFM, see: (d) Frommer, J. *Angew. Chem., Int. Ed. Engl.* **1992**, *31*, 1298. (e) Burnham, N. A.; Colton, R. J.; Pollock, H. B. *J. Vac. Sci. Technol. A* **1991**, *9*, 2548. (f) Weihs, T. P.; Nawaz, Z.; Jarvis, S. P.; Pethica, J. B. *Appl. Phys. Lett.* **1991**, *59*, 3536. (g) Meier, D. J.; Lin, F. *Langmuir* **1994**, *10*, 1660. (h) Rugar, D.; Hansma, P. *Physics Today* **1990**, *43(10)*, 23. (i) Quate, C. F. *Surf. Sci.* **1994**, *299/300*, 980.

(36) Liu, G.-Y.; Salmeron, M. B. *Langmuir* **1994**, *10*, 367.

(37) Hansma, H. G.; Gould, S. A. C.; Hansma, P. K.; Gaub, H. E.; Longo, M. L.; Zasadzinski, J. A. N. *Langmuir* **1991**, *7*, 1051.

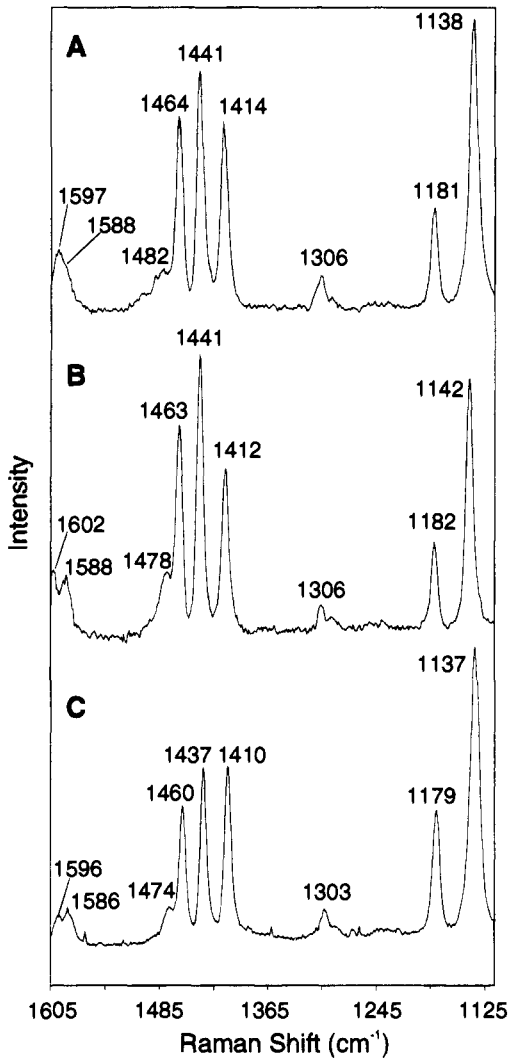

Figure 3. (A) Resonance Raman spectrum of **1a** in CH_2Cl_2. λ_{ex} = 501.7 nm, 160 mW, collection time = 10 s, 10 collections. (B) Resonance Raman spectrum of solid **1a**. λ_{ex} = 501.7 nm, 160 mW, collection time = 15 s, 20 collections. (C) SERS spectrum of a SAM of **1d** on Au(111)/mica. λ_{ex} = 752.1 nm, 35 mW, collection time = 60 s, 10 collections.

reconstructed Au surface or the S atoms attached to the substrate); at the same time they are too broad to be attributed to scattering from the entire molecule. The widths of the peaks in both rod scans (before and after annealing) correspond to a coherence thickness of ~10 Å, which suggests that the diffraction peak is due to ordering of only a portion of each adsorbate molecule that comprises the SAM. The maximum along the rod shifts to lower K_z after annealing, which indicates a change in the tilt of the ordered portion of the SAM. The width of the intensity distribution along the rod makes it impossible to determine precisely the tilt angle or direction of the ordered groups within the film, but we estimate they are originally tilted 20–30° before annealing and are approximately vertical afterwards.[35c] This is in contrast with the annealing behavior for SAMs of linear alkanethiols on Au(111), which show no irreversible structural changes of this type.[16b] The annealing process for the SAM of **1d** also results in a modest increase in the average domain diameter (or coherence length) from ~45 to ~55 Å. This also is in contrast with the annealing behavior for SAMs of linear alkanethiols on Au(111), which show at least a factor of 2 increase in the average domain diameter.[16b]

A Structural Model for a SAM of 1d on Au(111). Since the surface sensitive AFM studies of SAMs of **1d** on Au(111)/mica indicate a distorted hexagonal lattice with nearest-neighbor distances consistent with the XRD measurements, we conclude that both experiments are detecting the azobenzene portion of the film (estimated length ~10 Å, inset of Scheme 1) rather than the alkane tethering groups. In constructing a model for the structure of a SAM of **1d** on Au(111), we use the lattice parameter and orientation of the ordered groups obtained from the in-plane XRD experiment (4.50 ± 0.06 Å); the X-ray measurement is a more precise and less interactive one than AFM. For the azobenzene moieties to fit into the 4.50 Å lattice parameter, a herringbone structure must be adopted. Even though the monolayer is not commensurate with the substrate surface lattice (the intermolecular spacings are about 10% smaller than the $(\sqrt{3} \times \sqrt{3})R30°$ commensurate spacings), the SAM lattice orientation must be influenced by the substrate–molecule interaction since the lattice is rotated 30° with respect to the underlying Au(111) surface lattice as it is in the case for SAMs of linear alkanethiols on Au(111).[16a–c,36] This rotation suggests the S groups of **1d** chemically adsorb onto the Au(111) surface in a commensurate manner, perhaps at the same sites *n*-alkanethiols do on Au(111), which are 5.0 Å apart. From a chemical standpoint, this is quite reasonable, since (1) the chemistry involving thiol adsorption on Au(111) is identical and (2) the molecules do not substantially differ in their cohesive energies, which may be estimated from heat of fusion and heat of vaporization data. For **1d**, a summation of heat of fusion and heat of vaporization values[31] for an azobenzene moiety and undecane gives 1.5 eV/molecule, while a similar summation for octadecane gives 1.3 eV/molecule. Therefore, in such a model the azobenzene groups at the substrate/air interface must "condense" to form the more close-packed structure shown in Figure 9b, with the alkane chains tilting or bending to make this close approach possible. This condensation of the azobenzenes would lead to the domain size being dependent on the amount of bending the alkane chains could undergo. The average domain diameter for a SAM of **1d** on Au(111) is relatively small in comparison with SAMs of linear alkanethiols on Au(111) both before and after annealing.[16b] We estimate that after annealing the average domain in a SAM of **1d** consists of approximately 80 molecules. An idealized representation of the proposed structure, where small bundles of azobenzene groups make up the ordered domains in the monolayer, is given in Figure 11. A small domain size is consistent with our "bundle model"; as the domain size increases, the degree of alkyl bending necessary for the azobenzene groups to fit into the lattice also will increase. Substantial bending or tilting of the alkane chains is not necessary for the alkyl groups to be 5.0 Å apart near the Au (111) (as they would be for a commensurate structure on Au(111)) and the azobenzene moieties to be 4.50 Å apart. For an idealized SAM structure with 55 Å circular domains (~11 molecules along the diameter), through a trigonometric analysis we estimate that the edge adsorbate groups would have to bend only 11 degrees relative to the central adsorbate group in order to satisfy the 4.50 ± 0.06 Å lattice parameter. This assumes a vertical orientation of the azobenzene groups (i.e., the post-annealed structure) and a 30° tilt angle for the alkyl group of the central adsorbate molecule in the idealized domain. The tilt angle is the angle formed between the plane defined by the vertical azobenzene moiety (i.e., the surface normal) and the plane defined by the all *anti*- linear alkane chain.

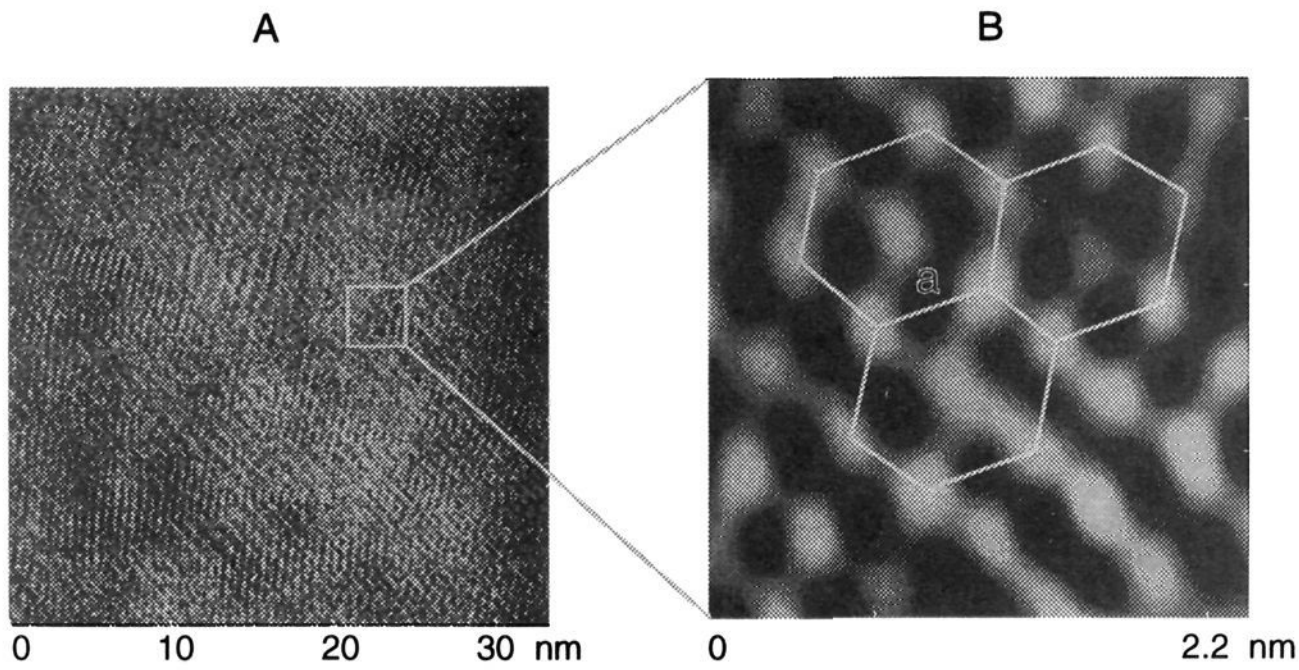

Figure 4. AFM images of a SAM of **1d** on Au(111)/mica. (A) A 33 nm × 33 nm scan size image. (B) A molecular resolution 2.3 nm × 2.3 nm image, showing a slightly distorted hexagonal lattice with a nearest neighbor distance of 4.6 Å. The image is spectrum filtered.

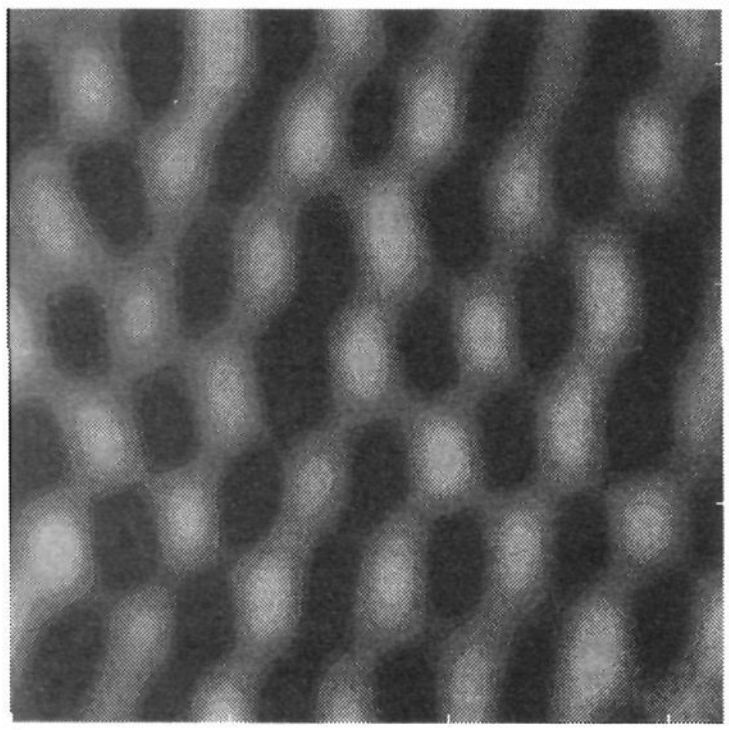

Figure 5. AFM image of a SAM of octadecanethiol on Au(111)/mica; nearest neighbor distance is 5.1 Å. The image is spectrum filtered.

Finally, it is not so surprising that a SAM of **1d** forms a herringbone structure rather than one that consists of face-to-face azobenzene dimers; the crystal structure of *trans*-azobenzene shows that even in the three-dimensional system, azobenzene orders in a herringbone pattern.[34] It should be noted that other workers, through molecular dynamics calculations and reflection-absorption IR spectroscopy, have proposed a herringbone structure for SAMs formed from two other aromatic molecule types, biphenyl and naphthalene.[38]

Electrochemistry of 1a and SAMs of 1d on Au(111)/Mica. Compound **1a** has electrochemical properties comparable to those reported for azobenzene.[39] In an aprotic medium such as THF, compound **1a** readily undergoes a reversible one-electron reduction to form a radical anion ($[PhN{=}NAr]^{\bullet -}$, Ph = C_6H_5, Ar = p-$C_6H_4O(CH_2)_{11}OH$, $E_{1/2} = -2.0$ V vs Fc/Fc^+), Figure 12a and eq 1.

The cyclic voltammetry for a SAM of **1d** on Au(111)/mica in THF/0.1 M Bu_4NPF_6 also exhibits a one-electron reduction/oxidation wave at $E_{1/2} = -2.0$ V vs Fc/Fc^+, Figure 12b. The surface coverage determination for **1d** from this electrochemical experiment is not straightforward. The integration of redox waves associated with surface-confined species has been used extensively as a method to determine adsorbate surface coverage for redox-active monolayer films.[1bc,14cd,23,40,41] In other work, we and others have shown that the accuracy of such a method is highly dependent upon the structure of the monolayer film and the ability for charge compensating ions to access the adsorbate species that are being oxidized or reduced.[21,40,42] The method determines adsorbate electrochemical accessibility and not necessarily adsorbate surface coverage. Therefore, given the densely packed structure for a SAM of **1d** and the upright orientation of the azobenzene groups within the SAM, it is not surprising that integration of the wave associated with the reduction of a SAM of **1d** yields an electrochemical accessibility of 1.9×10^{-11} mol/cm^2, which is substantially lower than the estimated adsorbate surface coverage for a full monolayer of **1d**. Assuming an upright orientation of the azobenzene groups, a hexagonal lattice with 5.0 Å nearest neighbor spacing,[43] and a substrate surface roughness factor of 1.35,[28a] the estimated surface coverage for a full monolayer of **1d** on Au(111)/mica is 1.0×10^{-9} mol/cm^2. From this calculation and a comparison with the experimentally determined electrochemical accessibility of surface-confined **1d**, we conclude that only ~2% of the azobenzene moieties in a SAM of **1d** are being electrochemically accessed in the cyclic voltammetry experiment.

Neither the AFM nor the in-plane XRD experiments provide information regarding macroscopic film density and uniformity. In-plane XRD only probes the ordered areas of the film, and AFM only samples microscopic areas of the surface. A significant consideration in determining the uniformity of a SAM formed from **1d** on Au(111) is its differential capacitance (C_d); the C_d of a SAM modified electrode has been cited as a measure

(38) (a) Chang, S.-C.; Chao, I.; Tao, Y.-T. *J. Am. Chem. Soc.* **1994**, *116*, 6792. (b) Sabatini, E.; Cohen-Boulakia, J.; Bruening, M.; Rubinstein, I. *Langmuir* **1993**, *9*, 2974.

(39) (a) Sadler, J. L.; Bard, A. J. *J. Am. Chem. Soc.* **1968**, *90*, 1979. (b) Boto, K. G.; Thomas, F. G. *Aust. J. Chem.* **1973**, *26*, 1251.

(40) Herr, B. R.; Mirkin, C. A. *J. Am. Chem. Soc.* **1994**, *116*, 1157.

(41) (a) Rowe, G. K.; Creager, S. E. *Langmuir* **1991**, *7*, 2307. (b) Katz, E.; Itzhak, N.; Willner, I. *Langmuir* **1993**, *9*, 1392. (c) Chen, K.; Caldwell, W. B.; Mirkin, C. A. *J. Am. Chem. Soc.* **1993**, *115*, 1193. (d) Chidsey, C. E. D.; Bertozzi, C. R.; Putvinski, T. M.; Mujsce, A. M. *J. Am. Chem. Soc.* **1990**, *112*, 4301.

(42) (a) Zhang, W.-X., Yahiro, H.; Mizuno, N.; Izumi, J.; Iwamoto, M. *Langmuir* **1993**, *9*, 2337. (b) Smith, C. P.; White, H. S. *Anal. Chem.* **1992**, *64*, 2398.

(43) 5.0 Å rather than 4.5 Å is used in this calculation since the spacing of the S end groups in our model rather than the azobenzene groups will determine the upper limit for the surface coverage of **1d** on Au(111).

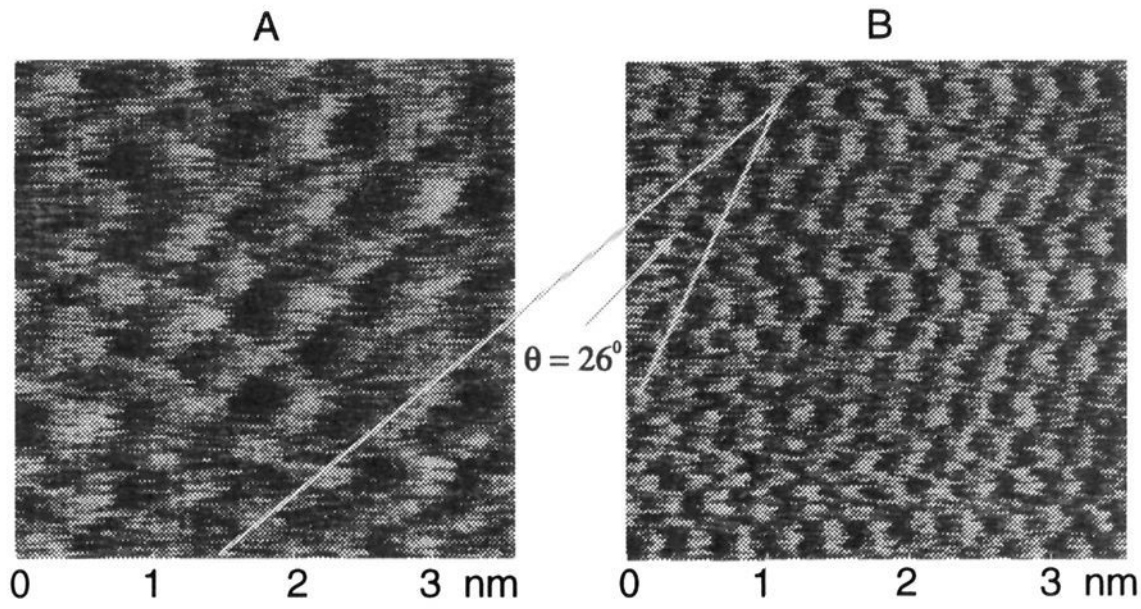

Figure 6. Force dependent AFM images of a SAM of **1d** on Au(111)/mica. (A) Image obtained with a total force ~15 nN. (B) Image obtained with a total force >300 nN.

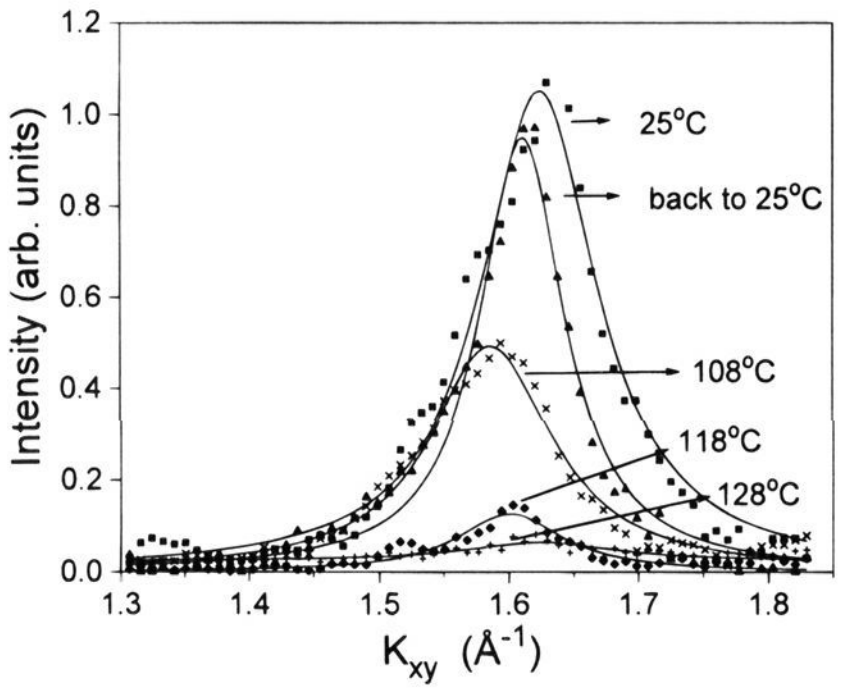

Figure 7. Radial diffraction scans at (■) 25 °C, $K_z = 0.45$ Å^{-1}; (×) 108 °C, $K_z = 0.45$ Å^{-1}; (◆) 118 °C, $K_z = 0.45$ Å^{-1}; (+) 128 °C, $K_z = 0.45$ Å^{-1}; (▲) back to 25 °C; $K_z = 0.15$ Å^{-1}. The solid lines are lorentzian fit to the data.

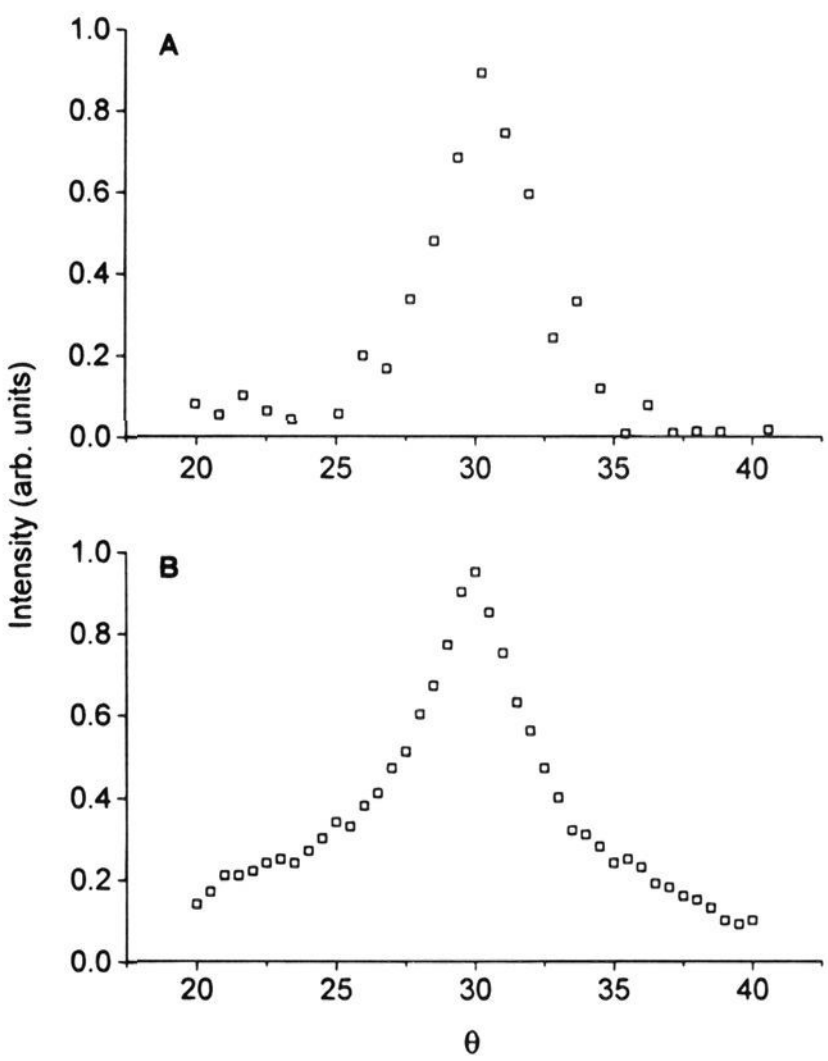

Figure 8. Rocking curves at the monolayer peak ($K_{xy} = 1.61$ Å^{-1}). $\theta = 0$ is the direction of one of the gold crystal truncation rods: (A) before annealing, $K_z = 0.45$ Å^{-1} and (B) after annealing, $K_z = 0.15$ Å^{-1}.

of ion permeability for a SAM.[32,44] For a modified electrode, the differential capacitance should decrease as film thickness increases and film permeability decreases. The measured differential capacitance ($C_{d,exp}$) for a SAM of **1d** at −0.1 V vs Ag wire is 1.6 μF/cm^2 and is within a factor of 2 of the theoretically predicted value ($C_d = 0.8$ μF/cm^2) calculated using the Helmholtz model, which treats the double layer as an ideal capacitor.[45] The disparity between the theoretical and experimentally determined C_d values could arise from error associated with our estimates of the refractive index, electrode area, and SAM thickness. In our hands, $C_{d,exp}$ for Au(111)/mica is 17.5 μF/cm^2, which is substantially greater than the SAM-modified substrates; therefore, interfacial capacitance data for Au(111)/mica modified with a SAM of **1d** is consistent with the formation of a densely packed monolayer film with uniform adsorbate coverage and thickness. If one compares this data with C_d data for SAMs of octadecanethiol on Au[32] and takes into account differences in film thickness and refractive index, the two SAMs are comparable at separating charge.

Further evidence of a densely packed SAM structure and uniform coverage for **1d** on Au(111)/mica comes from penetration studies of $Fe(CN)_6^{3-}$ (0.9 mM) in aqueous media. The cyclic voltammetry of $Fe(CN)_6^{3-}$ at an unmodified Au electrode exhibits a reversible wave at $E_{1/2} = 0.2$ V vs Ag wire, Figure 13a. The electrochemical response for a Au(111)/mica electrode modified with a SAM of **1d** in the same solution of $Fe(CN)_6^{3-}$ exhibits no detectable electroactivity associated with the $Fe(CN)_6^{3-}$ redox couple, Figure 13b, demonstrating that SAMs of **1d** are forming an impenetrable barrier to ions such as $Fe(CN)_6^{3-}$.

When the Au(111)/mica electrode modified with a SAM of **1d** is cycled through a potential that results in azobenzene reduction (−1.34 V) and then cycled through the potential window which effects $Fe(CN)_6^{3-}$ reduction/oxidation, a wave associated with the $Fe(CN)_6^{3-}$ redox couple begins to become apparent, Figure 13c. This is presumably a consequence of two factors: (1) increased disorder in the SAM that results from

(44) (a) Sabatani, E.; Rubinstein, I.; Maoz, R.; Sagiv, J. *J. Electroanal. Chem.* **1987**, *219*, 365. (b) Finklea, H. O.; Avery, S.; Lynch, M.; Furtsch, T. *Langmuir* **1987**, *3*, 409.

(45) Bard, A. J.; Faulkner, L. R. *Electrochemical Methods*, John Wiley & Sons: New York, 1980, Chapter 12.

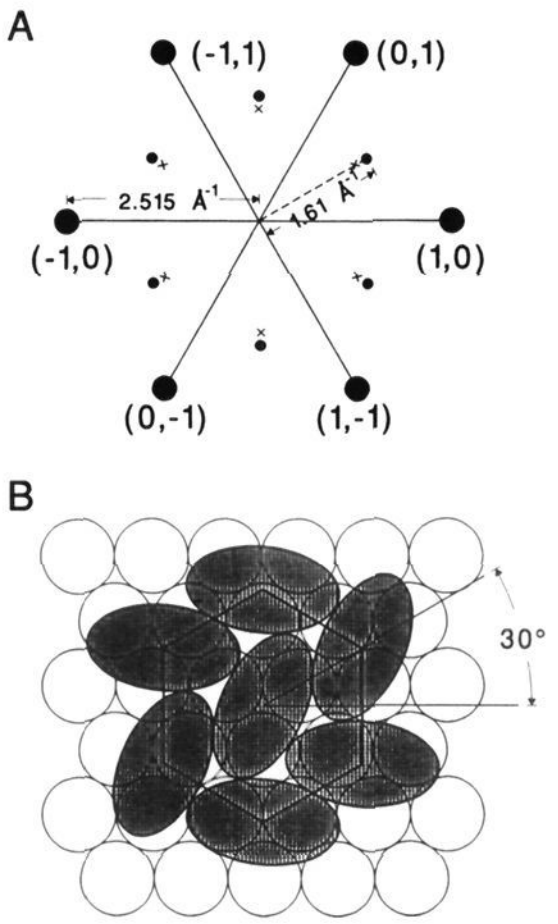

Figure 9. (A) Two-dimensional reciprocal space diagram showing Au crystal truncation rods (large circles) and monolayer diffraction peaks (small circles). The positions of the commensurate $\sqrt{3} \times \sqrt{3}$ R30° peaks are indicated by × for comparison. A hexagonal coordinate system has been used to index the Au rods.[33c] (B) Top view of a model of a Au(111) surface modified with **1d** showing gold atoms (open circles) and azobenzene molecules (filled ellipses) in an incommensurate hexagonal structure which illustrates the postulated herringbone arrangement of the azobenzene groups in a SAM of **1d**.

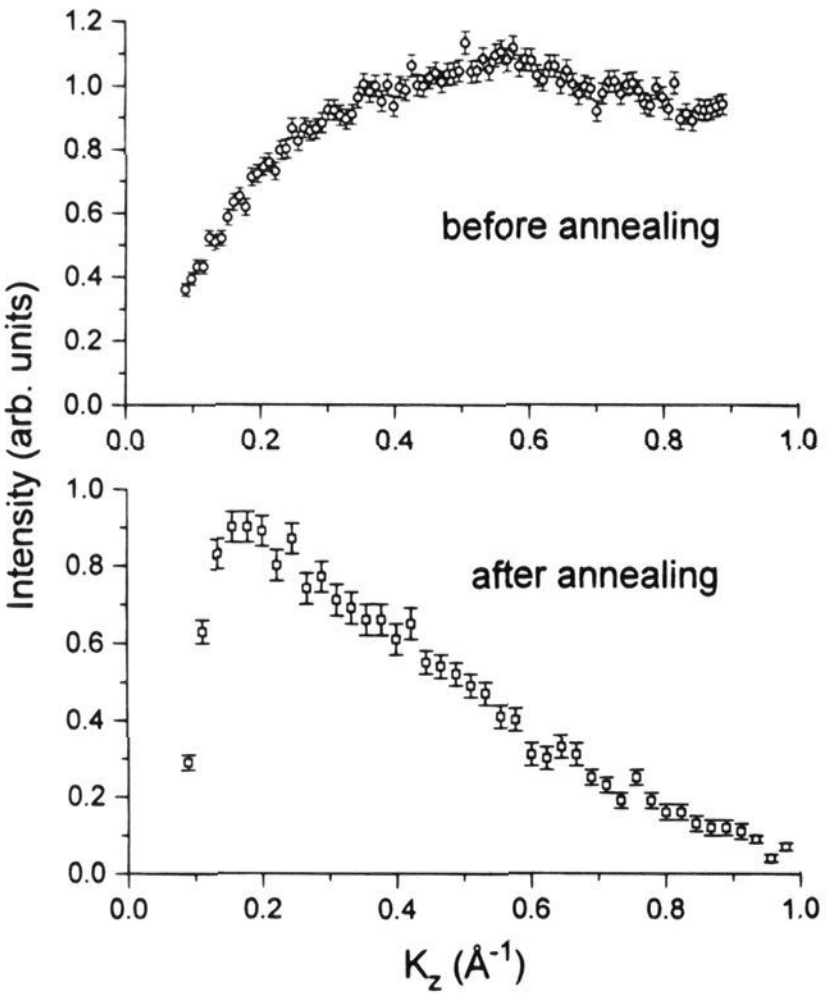

Figure 10. Rod scans at the observed monolayer diffraction peak position (K_{xy} = 1.61 Å^{-1}), at 25 °C before and after annealing.

moving ions in and out of the film during the electrochemical process and (2) desorption of some of the adsorbed thiolate species from the electrode surface, which introduces free volume into the monolayer structure. Monolayers prepared from alkanethiols adsorbed on Au(111) may be electrochemically

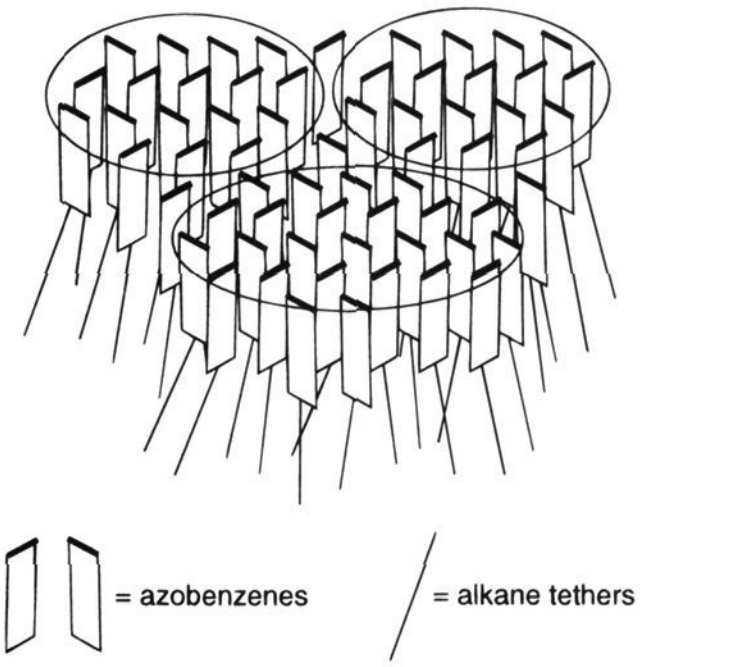

Figure 11. A drawing depicting the "bundle model" for a SAM of **1d** on Au(111). In this model, the azobenzene groups are spaced 4.5 Å apart and the S atom end groups are spaced 5.0 Å apart. The alkyl groups tilt inward so that the azobenzene groups may pack in a hexagonal lattice. Domains are indicated by the large circles. Adsorbate molecules that are not part of the ordered domains may disperse themselves randomly at the interfaces of the ordered domains.

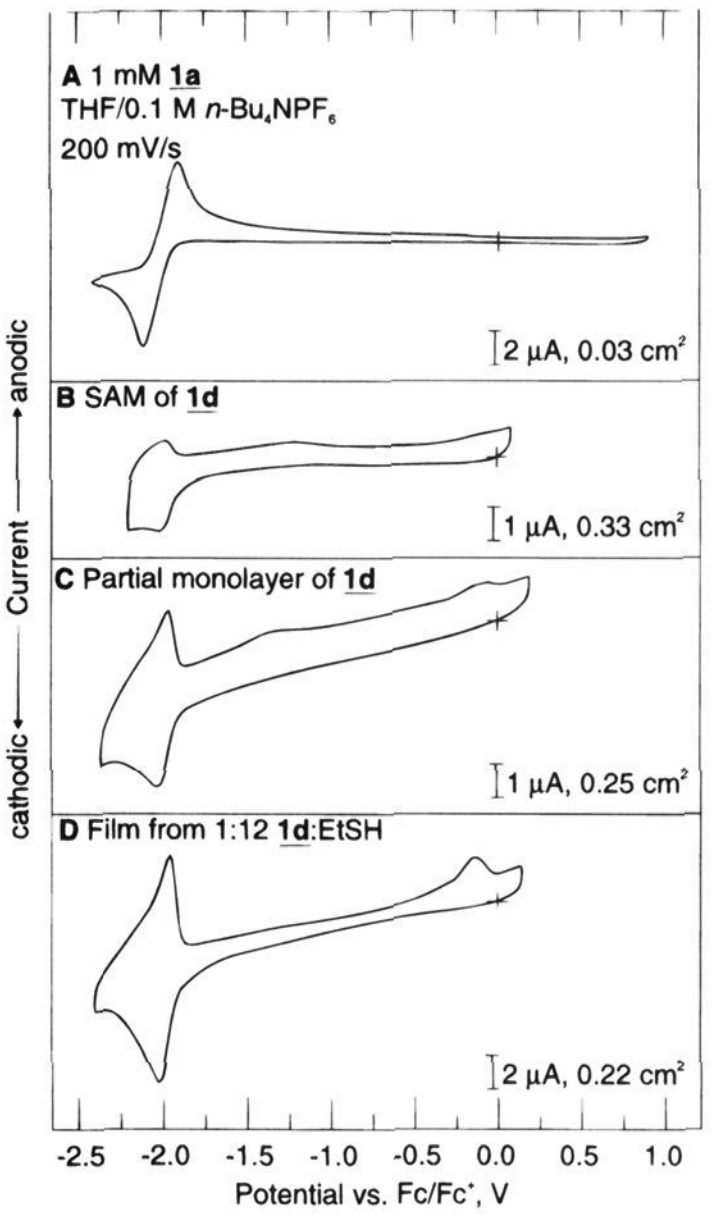

Figure 12. Cyclic voltammetry for (A) **1a** at a Au disk electrode, (B) a SAM of **1d** on Au(111)/mica, (C) **1d** on Au(111)/mica at submonolayer coverage (5 min immersion), and (D) **1d** coadsorbed with ethanethiol in a 1:12 ratio. A THF/0.1 M n-Bu_4NPF_6 electrolyte was used for all electrochemical measurements.

desorbed in H_2O/0.2 M $NaClO_4$ at potentials comparable to those used to effect azobenzene reduction (−1.34 V for octadecanethiol on Au(111)/mica). Others have demonstrated that monolayers prepared from alkanethiols may be electrochemically desorbed from Au(111) in a variety of protic and

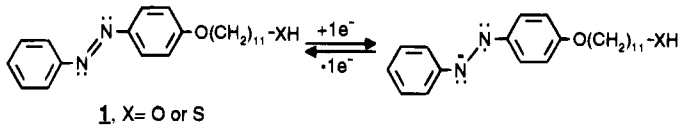

(1)

1, X= O or S

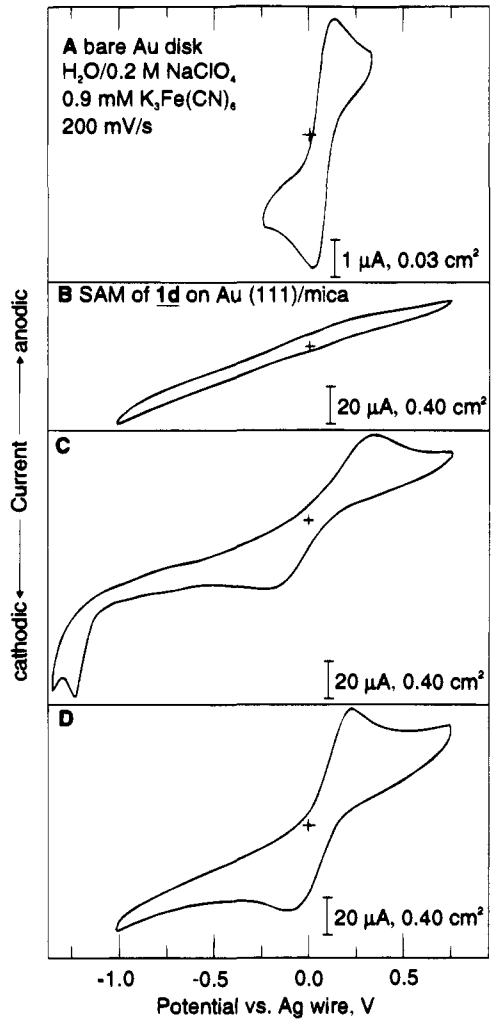

Figure 13. Cyclic voltammetry for 0.9 mM $K_3Fe(CN)_6$ in H_2O/0.2 M $NaClO_4$ (A) at a bare Au disk electrode, (B) at a SAM of **1d** on Au(111)/mica, (C) at the same SAM after cycling to −1.34 V, and (D) at the same SAM after repeated cycling to −1.34 V.

aprotic media.[46] As the electrode modified with a SAM of **1d** is cycled repeatedly between −1.34 V and 0.70 V, the anodic peak-to-cathodic peak separation of the $Fe(CN)_6^{3-}$ wave continues to decrease, indicating that the film is becoming more penetrable as a result of the electrochemical cycling process, Figure 13d. A similar, although less pronounced, effect is observed when the reductive side of the potential window is decreased to −1.00 V (i.e., at a potential that does not result in the reduction of the surface bound azobenzene groups or desorption of the monolayer) indicating that the film becomes more penetrable as ions are moved to and from the electrode surface.

The Electrochemical Accessibility of 1d on Au(111)/Mica. The electrochemical accessibility of **1d** should depend on the amount of free volume in the SAM; increased free volume should result in increased electrochemical accessibility for **1d**. There are two ways to incorporate free volume into a monolayer film prepared from **1d** on Au(111)/mica: (1) shorter immersion times and (2) coadsorption of **1d** with a short chain linear alkanethiol such as ethanethiol. For example, a Au(111)/mica substrate soaked in a 1 mM cyclohexane solution of compound **1d** for only 5 min exhibits a different response than those soaked for 48 h, compare Figure 12c with 12b. The electrochemical accessibility of azobenzene groups for films prepared in the former manner (7.1×10^{-11} mol/cm^2, 7% of a monolayer) is greater than for ones prepared in the latter manner (2%). The current associated with oxidation of the azobenzene radical anion is slightly lower than the current associated with azobenzene radical anion formation because some of the radical anion is converted to hydrazobenzene, the two electron, two proton reduction product, eq 2; the oxidation of the hydrazobenzene occurs at −0.1 V vs Fc/Fc^+, Figure 12c. The radical anion is extremely sensitive to H^+, and trace amounts of H_2O or other H^+ sources can lead to hydrazobenzene formation.[39a,40]

If Au(111)/mica is soaked in a 1:12 cyclohexane solution of **1d** and ethanethiol for 18 h, rinsed, and studied by cyclic voltammetry, the electrochemical accessibility of the azobenzene groups is significantly enhanced (2.7×10^{-10} mol/cm^2, 27% of a SAM of pure **1d**) as compared with the SAM of pure **1d**, compare Figure 12d with 12b. Note a small amount of hydrazobenzene also is formed in this experiment. These experiments strongly suggest that the structure of the SAM is inhibiting the incorporation of charge compensating n-Bu_4N^+ ions into the film, which is necessary for azobenzene reduction to be effected at potentials that result in reduction of solution azobenzene. This is consistent with the experimental observations we have made for monolayer films of ferrocenylazobenzene and fullerene capped alkanethiols adsorbed on Au(111).[21,40] This is a critical issue with regard to the characterization and evaluation of redox-active monolayers; many arguments made throughout the literature rely on surface coverages for adsorbate molecules that are determined by cyclic voltammetry.[1b,c,14c,d,23,40,41] Clearly, for some systems, including **1d** on Au(111), electrochemically determined surface coverage will be substantially lower than actual adsorbate surface coverage. The scope of this phenomenon has yet to be determined.

Summary of Electrochemical Experiments. These electrochemical experiments demonstrate the following: (1) SAMs of **1d** on Au(111) are uniform densely packed structures, (2) electrochemical cycling, even in a potential window that does not effect adsorbate electrochemistry, significantly affects film structure (in this case increases monolayer porosity), and (3) the electrochemical accessibility of the adsorbate species in these SAMs is *not* necessarily a reflection of the adsorbate surface coverage; in fact, these experiments show that only a small fraction of the azobenzene groups within a SAM of **1d** may be reduced in a potential window that results in the reduction of solution **1a**.

Conclusions

We have detailed the preparation and structural characterization of a SAM formed from a new surface-confineable azobenzene-containing molecule, **1d**, on Au(111). We have utilized AFM and synchrotron in-plane XRD experiments to unequivo-

(46) (a) Widrig, C. A.; Chung, C.; Porter, M. D. *J. Electroanal. Chem.* **1991**, *310*, 335. (b) Schneider, T. W.; Buttry, D. A. *J. Am. Chem. Soc.* **1993**, *115*, 12391. (c) Walczak, M. M.; Popenoe, D. D.; Deinhammer, R. S.; Lamp, B. D.; Chung, C.; Porter, M. D. *Langmuir* **1991**, *7*, 2687. (d) Weisshaar, D. E.; Lamp, B. D.; Porter, M. D. *J. Am. Chem. Soc.* **1992**, *114*, 5860.

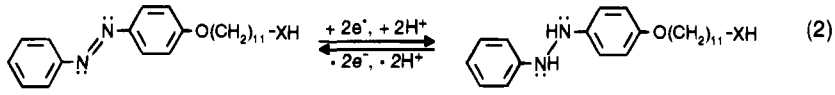

(2)

1, X= O or S

cally show that this SAM is a highly ordered structure and have proposed a new "bundle model" to describe that structure. The "bundle model" consists of small domains of ordered azobenzene groups resting over surface-adsorbed, inward tilting alkyl tethering groups. It suggests that the azobenzene group, although not completely independent from Au(111) surface influence, plays a large role in dictating the overall monolayer structure. The propensity for the azobenzene group to form the contracted structure illustrated in Figure 9b demonstrates the utility of the azobenzene group as a new structural motif for highly ordered SAMs. We also have shown that a SAM of **1d** undergoes an irreversible structural change at high temperatures, which involves a change in tilt angle for the ordered azobenzene units that comprise the SAM. This is an unprecedented phenomenon and shows that SAMs can form both kinetic and thermodynamic ordered structures. SAMs of **1d** are uniform and impenetrable to $Fe(CN)_6^{3-}$ ions in aqueous solution, and the redox-activity of the surface-confined azobenzene moiety has been shown to be dependent upon monolayer structure. The latter observation underscores the importance of understanding the relationship between monolayer structure and electron transfer processes. In general, understanding the factors that control SAM formation for adsorbate molecules which contain electro-, photo-, and chemically reactive functionality ultimately will provide greater predictability of the chemical and physical properties of materials constructed from SAM methodology.

Acknowledgment. C.A.M. acknowledges the Office of Naval Research (URI3136YIP) and the National Science Foundation (CHE-9121859) for support of this work. P.D. and C.A.M. also acknowledge support by the MRSEC Program of the National Science Foundation, at the Materials Research Center of Northwestern University, under Award No. DMR-9120521. B.R.H. and W.B.C. are grateful for ARCS Foundation Fellowships. B.R.H. also acknowledges a Henkel Corporation Research Fellowship, and M.K.D. is grateful for an AT&T Bell Laboratories Ph.D. Scholarship. Work performed at the ANL X6B beam line is supported by the DOE Contract No. W-31-109-ENG-38.

Supplementary Material Available: Fourier transforms for the AFM images of a SAM of **1d** and a SAM of octadecanethiol and experimental synthetic details for **1a−d** (5 pages). This material is contained in many libraries on microfiche, immediately follows this article in the microfilm version of the journal, can be ordered from the ACS, and can be downloaded from the Internet; see any current masthead page for ordering information and Internet access instructions.

JA943571Y